From single molecules to water networks: dynamics of water adsorption on Pt(111)

Maryam Naderian[1,*] and Axel Groß[1,†]

[1] *Institute of Theoretical Chemistry, University of Ulm, Albert-Einstein-Allee 11, D-89069 Ulm, Germany*

(Dated: May 23, 2016)

The adsorption dynamics of water on Pt(111) was studied using ab initio molecular dynamics (AIMD) simulations based on density functional theory calculations including dispersion corrections. Sticking probabilities were derived as a function of initial kinetic energy and water coverage. In addition, the energy distribution upon adsorption was monitored in order to analyze the energy dissipation process. We find that on the water pre-covered surface the sticking probability is enhanced because of the attractive water-water interaction and the additional effective energy dissipation channels to the adsorbed water molecules. The water structures forming directly after the adsorption on the pre-covered surfaces do not necessarily correspond to energy minimum structures.

I. INTRODUCTION

Properties of water/metal interfaces are of tremendous technological importance as they influence processes in, e.g., electrocatalysis, electrochemical energy conversion and storage, and corrosion [1–3]. At the same time, they are very interesting from a fundamental point of view since they are governed by a delicate interplay between metal-water and water-water interaction [4] which are of comparable strength [5, 6]. Because of this importance, the adsorption of water monomers, clusters, and layers on metal surfaces has been studied extensively both from a experimental [1–3, 7–11] and a theoretical point of view [5, 10–24].

These studies have typically focused on structural aspects of water/metal interfaces. Water is the smallest molecule that can form extended hydrogen-bonded networks. However, the study of dynamical aspects in the water-metal interaction is also very interesting as it provides additional insights into the factors underlying the structure formation of water on metal surfaces. It is important to note that water adsorbs intact on many metal surfaces such as Pt, Cu or Ag [5]. This means that the adsorption probability on these surfaces is determined by energy transfer and dissipation processes [25] which depend on the mass ratio between the impinging molecule and the atoms and molecules on the surface. Consequently, on a water-precovered metal surface, the metal atoms and the pre-adsorbed water molecules might play a rather different dynamical role in the adsorption process due to their mass difference in spite of the fact that the water-metal and the water-water interaction are of comparable strength.

Recently, Campbell and coworkers [26] measured the sticking probability of water on Pt(111) and the heat of adsorption as a function of the water coverage using calorimetric measurements. They observed that the sticking probability increases with increasing water coverage; for coverages higher than roughly 3/4 of a monolayer it stays constant at a value close to one [26]. It was also shown that increasing the temperature leads to a decrease in the sticking probability at low water coverages. These findings with respect to the sticking probability are in good agreement with similar data obtained by Haq *et al.* [27]. The heat of water adsorption stays roughly constant at about 0.56 eV for coverages up to about 0.6 monolayers (ML) with an slight increase which has been interpreted as being due to the water-water attraction through hydrogen bonding [26].

As far as theoretical studies of the adsorption dynamics of water on Pt surfaces are concerned, to the best of our knowledge we are only aware of a molecular dynamics study of water adsorption on $Pt\{110\}-(1\times2)$ based on a parameterized potential with the water-metal interaction derived from density functional theory (DFT) calculations [28, 29]. However, the substrate was kept fixed so that the energy transfer to the substrate necessary for sticking had to be modeled by using different thermostat schemes. Only by assuming that the energy dissipation increases exponentially with the total energy of the impinging molecules, the initial increase of the sticking probability for $H_2O/Pt\{110\}-(1\times2)$ observed in the experiment [30] could be reproduced.

There is no simple analytical interpolation scheme that describes the water-water, the water-metal, and the metal-metal interaction at the same time [31]. Hence a quantum chemical approach is needed for a reliable description of the whole system. Therefore, in order to elucidate the adsorption dynamics of water on Pt(111), we have performed ab initio molecular dynamics (AIMD) simulations based on density functional theory (DFT) calculations within the generalized gradient approximation (GGA) [32] for the description of exchange-correlation effects. Dispersion corrections were included in the DFT calculations as they are necessary to reliably describe the water-water and water-metal interaction [18, 20, 21, 23, 24, 33, 34] when using GGA functionals.

First we will address the adsorption dynamics of H_2O on clean Pt(111) and particularly focus on the

* Maryam.Naderian@uni-ulm.de
† axel.gross@uni-ulm.de

energy redistribution upon the impinging of the water molecule. Then we will discuss water adsorption on water-precovered surfaces and relate or findings to the measured sticking probabilities as a function of coverage, but we will also analyze the initial steps in the water network formation process on a metal surface.

II. COMPUTATIONAL METHODS

AIMD simulations were performed based on periodic DFT calculations using the Vienna ab initio simulation package (VASP) [35]. The exchange-correlation effects were described by using the generalized gradient approximation (GGA) with the revised PBE-functional of Hammer et al. (RPBE) [32]. The optimized lattice constant calculated for Pt using the RPBE functional is 3.99 Å which compares satisfactorily with the experimental value of 3.92 Å. As the consideration of dispersion is necessary in order to reproduce the water-water and water-metal interaction properly [18, 20, 21], they were taken into account through the D3 correction scheme of Grimme *et al.* [36]. The RPBE-D3 scheme has been shown to give a very reliable description both of the wetting behavior of water on metal surfaces [20] as well as of the properties of liquid water, water clusters and bulk ice [24, 33]. The screening of the dispersion interaction within the metal was approximated by considering the dispersion correction only for the uppermost layer of the slab, as suggested in Refs. [37, 38].

Electron-core interactions are accounted for by the projector augmented wave method [39, 40]. An energy cutoff of 400 eV was chosen in the electronic one-particle wave function expansion in order to achieve a sufficient size of the plane-wave basis set. The metal surface was modeled by a five atomic layers slab that were separated by a vacuum region of about 16 Å. The adsorption dynamics on Pt(111) were determined using a 3×3 surface unit cell. A k-points sampling of 3×3 turned out to be sufficient as an approximation to the integration over the first Brillouin zone.

The molecular dynamic simulations were performed using the Verlet algorithm with a time step of 1 fs in the microcanonical ensemble, i.e., the total energy of system was conserved along the trajectories. The trajectories were started above the surface at a distance of 5 Å from the uppermost Pt layer where the potential energy surface is uniform in the lateral degrees of freedom. For the case of water-precovered Pt(111) the trajectories were started at a distance of 9.5 Å from the uppermost Pt layer to avoid any water-water interaction in the initial conditions.

A relaxed configuration of the water molecule was used as an initial configuration, the initial orientation was randomly chosen using the quaternion method, and the lateral center of mass position was varied randomly. The vibrational zero-point energy was not taken into account in the initial conditions based on the assumption that the sum of all zero-point energies stays approximately constant along the adsorption path [41]. The sticking probabilities were derived by averaging over $N = 100$ trajectories leading to a statistical error of the sticking probability of $\sigma = \sqrt{s(1-s)/N} \leq 0.05$ where s is the adsorption probability [42]. The sequence of random initial conditions were kept the same for all initial kinetic energies so that trajectories at different kinetic energies with the same initial conditions can be compared.

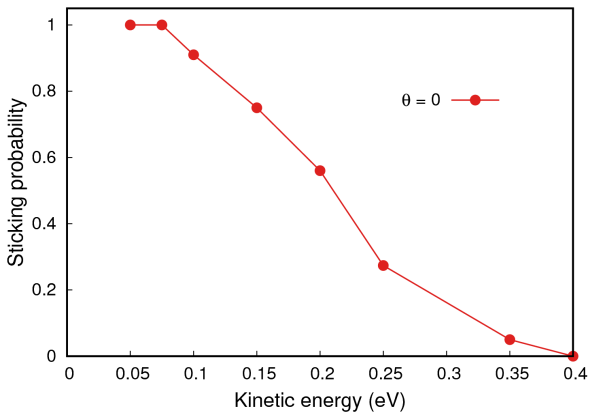

FIG. 1. Sticking probability on clean Pt(111), as a function of the initial kinetic energy of the impinging water molecule, is statistically averaged over all adsorption events (red points).

The formation energy of a water network per molecule with n molecules per surface unit cell is given by

$$E_{\mathrm{nH_2O/Pt}} = (E_{\mathrm{total}} - E_{\mathrm{slab}} - nE_{\mathrm{H_2O}})/n \ , \qquad (1)$$

where E_{total} is the energy of the total system, E_{slab} the energy of the clean Pt(111) slab and $E_{\mathrm{H_2O}}$ the energy of one water molecule in the gas phase. Note that the negative value indicates an energy gain upon adsorption and positive values correspond to repulsion.

In order to discuss the formation of the water network, we define the differential adsorption energy by

$$E_{\mathrm{diffads}} = E_{\mathrm{(n+1)H_2O/Pt}} - E_{\mathrm{nH_2O/Pt}} - E_{\mathrm{H_2O}}. \qquad (2)$$

which corresponds to the adsorption energy of a water molecule that is added to a water-precovered surface with n water molecules per surface unit cell.

III. RESULTS AND DISCUSSION

A. Sticking probability and dynamics of single molecule adsorption

First we determined the sticking probability of a water molecule impinging on a clean Pt(111) surface as a function of the kinetic energy. As Fig. 1 demonstrates, for water molecules with a kinetic energy ≤ 0.075 eV, the sticking probability is unity, and then it drops with increasing kinetic energy. At $E_{\mathrm{kin}} = 0.1$ eV, still 93% of the

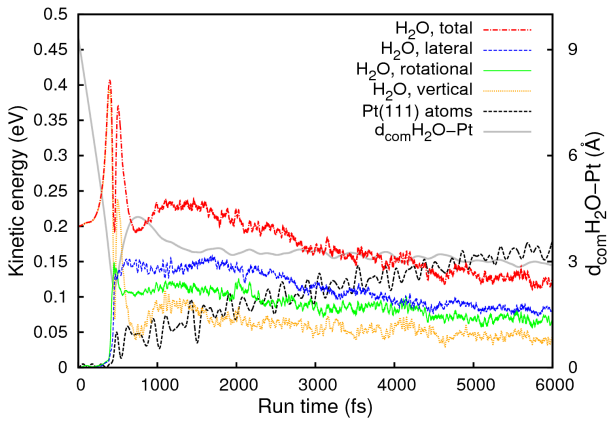

FIG. 2. Energy redistribution upon water adsorption on clean Pt(111) averaged over 100 trajectories for an initial kinetic energy $E_{\rm kin} = 0.2$ eV: total kinetic energy of the water molecule (red chain), lateral translational (blue dashed), rotational (green dashed thin) and vertical (orange dots) kinetic energy. Additionally, the kinetic energy of the Pt(111) atoms (black dashed thick) and the center-of-mass distance of the water molecule from the surface (gray solid) is plotted.

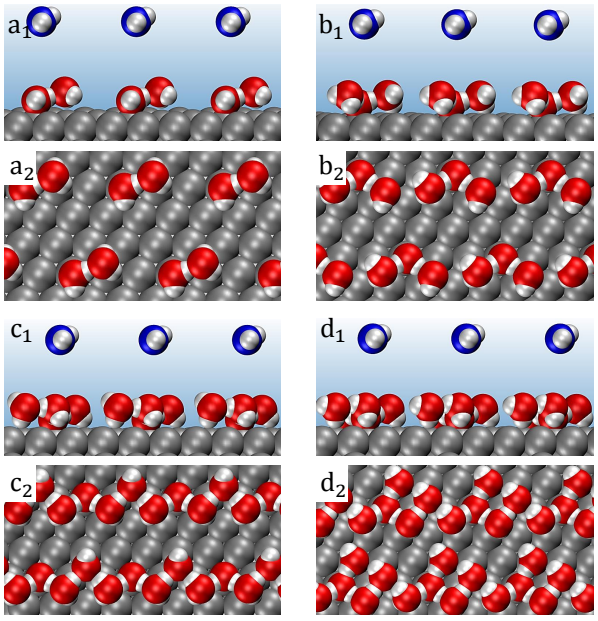

FIG. 3. (Side and top views of the lowest energy structures for water coverages 2/9, 1/3, 4/9 and 5/9 on Pt(111) within a 3×3 geometry that has been used as the initial conditions for the determination of the water sticking probabilities at water-precovered Pt(111).

incident water molecules adsorb, but at $E_{\rm kin} = 0.35$ eV, only 5% stick. Such an energy dependence of the sticking probability is expected for molecular adsorption with the molecule staying intact [43]: Sticking requires energy transfer from the impinging molecule to the substrate which becomes less efficient for higher kinetic energy.

In order to understand the water adsorption process in more detail, we have monitored the energy transfer into the molecular and substrate degrees of freedom along the trajectories. The different contributions for an initial kinetic energy $E_{\rm kin} = 0.2$ eV are plotted in Fig. 2. The vibrational motion of the water molecule correspond to the fastest degrees of freedom, therefore they follow the adsorption process almost adiabatically [41] so that the energy transfer into vibrations is negligible and not plotted in Fig. 2.

The water molecule starts moving toward the surface from a distance of 5 Å above the Pt slab. After 450 fs, it enters the attractive potential well at the surface illustrated by the gain in kinetic energy of about 0.2 eV. Note that this energy gain does not correspond to the binding energy of a water molecule on Pt(111) of 0.45 eV as this energy gain corresponds to an average and in general the water molecules do not hit the surface in the energetically most favorable adsorption geometry. At 750 fs the water molecule hits the repulsive wall of the water-Pt interaction. The following scenario is rather similar to the one that has been described for the molecular adsorption of O_2 on Pt(111) [25]. Upon the first encounter, some energy is transfered to the Pt atoms, but not enough to keep the molecule at the surface. However, there is a significant energy transfer to the lateral and rotational degrees of freedom of the water molecule. These energy is then not available to scatter back into the gas phase so that the water molecule cannot leave the adsorption well. The molecule bounces back and forth in this well and thus continues to transfer energy to the substrate. However, this process is rather slow due to two factors: the large mass mismatch between the water molecule and the Pt atom, and the relative weak water-metal interaction. Even after more than $t = 5$ ps the molecule is not fully equilibrated but still loses energy to the Pt substrate.

An analysis of the trajectories yields that at $t = 6$ ps almost 50% of the water molecules are positioned at the most favorable adsorption site, the top site with an adsorption energy of $E_a = -0.45$ eV. The average distance of the water molecule center of mass at the top sites from the Pt surface is d_{com}H$_2$O-Pt$=$ 2.7 Å whereas the energy minimum distance is 2.48 Å indicative of the vibrational center-of-mass and rotational motion of the water molecule in the adsorption well.

B. Step by step from dimerization to water bilayer

Next we address the adsorption of water on precovered surfaces. For water coverages of 1/9, 2/9, 1/3, 4/9 and 5/9 we determined the energy minimum adsorption structures which are shown in Fig. 3. For these coverages, we derived sticking probabilities for initial kinetic energies of 0.05 and 0.2 and for coverages 1/9, 2/9 and 5/9 the sticking probability at $E_{\rm kin}$ =0.4 eV is calcu-

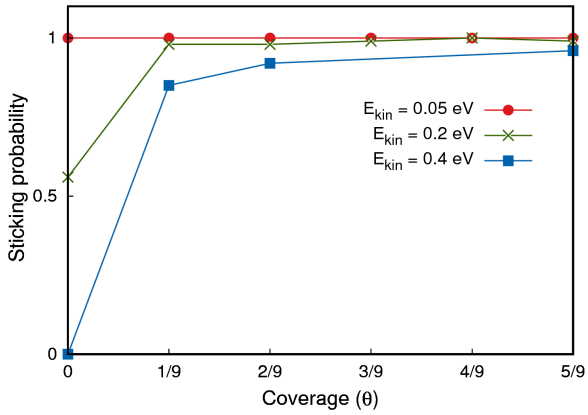

FIG. 4. Sticking probability as a function of water coverage for three different initial kinetic energies of the impinging water molecules, $E_{\rm kin}$ = 0.05 (red), $E_{\rm kin}$ = 0.2 (green) and $E_{\rm kin}$ = 0.4 (blue).

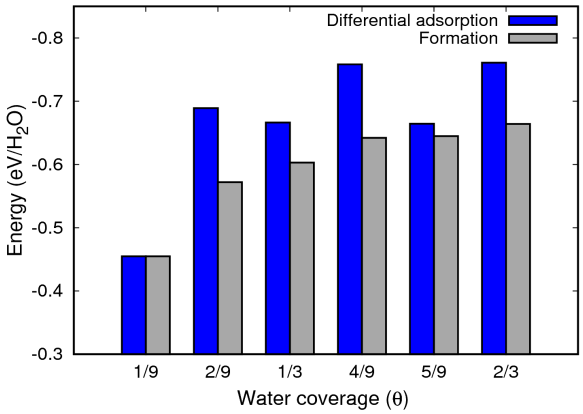

FIG. 5. The total and the differential water adsorption energy per water molecule according to Eqs. 1 and 2, respectively, as a function of coverage.

lated, Fig. 4. For all considered water pre-covered surfaces the sticking probability at $E_{\rm kin}$ =0.05 eV is unity. At $E_{\rm kin}$ =0.2 eV, the sticking probability increases from 52% for clean Pt(111) to 98% for the surface with one pre-adsorbed water molecule per 3×3 surface unit cell and then stays roughly constant close to unity. Further increasing the kinetic energy to $E_{\rm kin}$ =0.4 eV reduces the sticking probability to zero at the clean surface which rises to 96% for the surface with a water coverage 5/9.

This means that at kinetic energies of 0.2 eV and 0.4 eV the presence of pre-adsorbed water molecules leads to an increase in the sticking probability. This is in qualitative agreement with the experiment [26]. Still, there is a reduction in the sticking probability at all coverages with increasing kinetic energy. It has to be noted that our results cannot be quantitatively compared with the experiment as we only consider one particular water adsorbate structure per coverage, namely the energy minimum structure within a 3×3 surface unit cell at a given coverage, whereas in the experiment a statistical distribution of water structures exists. Sticking probabilities on precovered surfaces can sensitively depend on the particular structure of the adsorbed species [44]. Still, the qualitative trends obtained in our simulations should still be relevant in the comparison with the experiment.

To get a better understanding of the origin for the enhancement of the sticking probability at higher coverages, we have first analyzed the energetics of water adsorption. Fig. 5 shows the total and differential adsorption energy per water molecule according to Eqs. 1 and 2, respectively, as a function of coverage. For all pre-covered surfaces, the differential adsorption energy is larger than the total adsorption energy, for example by 0.25 eV upon the formation of a water dimer on Pt(111). This of course reflects the attractive water-water interaction due to hydrogen bond formation. Often, small adsorbates exhibit a repulsive interaction due to dipole-dipole interaction [45, 46]. This is different in water adsorption

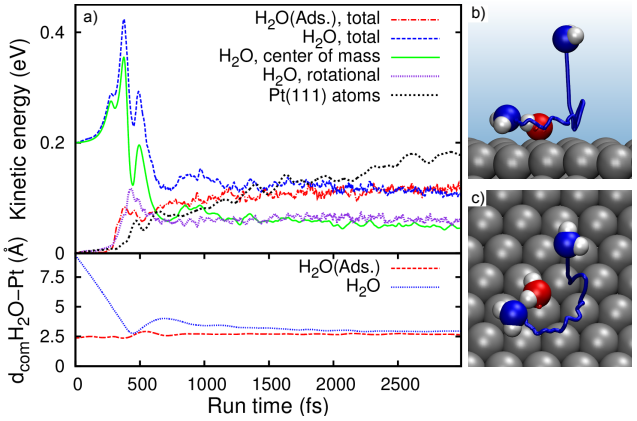

FIG. 6. Water adsorption on Pt(111) with a water coverage of 1/9 and an initial kinetic energy of $E_{\rm kin}$ = 0.2 eV. Left panel: Energy redistribution upon water adsorption, averaged over 100 trajectories, into the degrees of freedom of the impinging and the adsorbed water molecule and the Pt substrate. Right panels: Illustration of the adsorption process using a typical trajectory.

on metal surfaces. The favorite adsorption configuration of the water dimer, e.g., is determined by a competition between the most favorable water-Pt interaction at the top site and the formation of the hydrogen bond with the other water molecule. Such an additional attractive interaction between adsorbates necessarily leads to a higher sticking probability [47].

However, the pre-adsorbed water molecule also plays an important role as an efficient additional energy dissipation channel which is also crucial for the molecular adsorption [44]. This is illustrated in Fig. 6a where the energy distribution upon water adsorption on Pt(111) with a water coverage of 1/9 and an initial kinetic energy of $E_{\rm kin}$ = 0.2 eV averaged over 100 trajectories is shown.

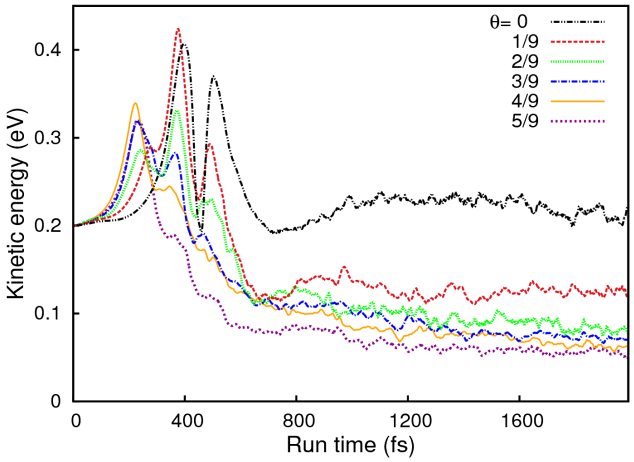

FIG. 7. Average total kinetic energy as a function of run time of a H_2O adsorbing on Pt(111) with water coverages from 0 to 5/9 for an initial kinetic energy of $E_{\rm kin} = 0.2$ eV.

In addition, one typical trajectory is shown in panels b and c, which illustrates our observation from the AIMD runs that at a water coverage of 1/9 all impinging water molecules are steered toward the pre-adsorbed water molecule.

As Fig. 6a demonstrates, upon impinging on the surface, the initial energy transfer to the pre-adsorbed water molecule is much larger than to the Pt substrate atoms. This can be easily understood considering the mass difference between the water molecule and the Pt atoms which makes the energy transfer to the pre-adsorbed water molecule much more efficient. Still, also the energy redistribution from the translational to the rotational degree of freedom is significant and important for the sticking. After about 2 ps, the total kinetic energies of the impinging and the pre-adsorbed molecules are the same indicating that the two water molecules have equilibrated their surplus energy upon the adsorption of the second water molecule among each other.

The water trajectory shown in Fig. 6b and c indicates that the impinging water molecule follows a semi-circle around the pre-adsorbed water molecule which stays at the ontop position. This is a consequence of the specific impact conditions. For other initial conditions a joint lateral movement of both water molecules has also been observed.

Raising the surface water coverages increases the probability that a pre-adsorbed water molecule is directly hit by an impinging molecule. Furthermore, it makes the energy transfer more efficient as the excess energy upon adsorption can be spread among more water molecules. This is illustrated in Fig. 7 were the average total kinetic energy of the adsorbing water molecule is compared for water coverages from zero to 5/9. The higher the coverage, the faster the adsorbing molecule dissipates its energy. For lower coverages, the initial bounces of the water

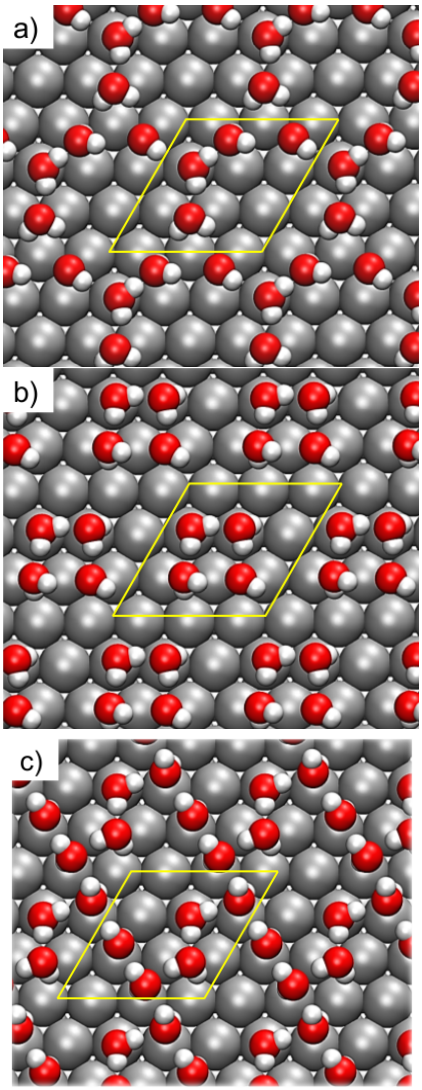

FIG. 8. Most frequent intermediate structural configurations forming for water impinging on water pre-covered Pt(111) with an initial coverage of $\theta = 3/9$ (panels a and b) and $\theta = 4/9$ (panel c).

molecule on the surface are clearly visible in its kinetic energy, but they are hardly discernible for the highest coverage of 5/9. This illustrates the very efficient energy transfer from the impinging water molecule to the water layer.

We will now discuss the adsorption dynamics of the water molecules on the surface at higher water coverages in more detail. Here we do not discuss the energy minimum structures that should eventually be formed, but the typical structural motifs that develop dynamically during the adsorption process on water-precovered Pt(111) at the structures illustrated in Fig. 3. A water molecule impinging on Pt(111) with one water dimer per 3×3 surface unit cell quickly forms a water trimer, faster than the dimer formation occurs on a surface covered by water monomers. The most stable trimer structure

consists of a bent arrangement, similar to the structure shown in Fig. 3b. The central atom is located with its oxygen atom above a Pt ontop site. The other two water molecules are slightly tilted so that the height of their oxygen atoms is a little bit larger than the one of the central water molecule. We find an asymmetric configuration of the non-central water molecules which might be caused by the interaction with the periodic images.

When the Pt(111) is covered by water trimers in a 3×3 surface unit cell at a coverage of 3/9, in principle two different patterns are possible. Either the water molecules form some kind of extended network structures or an arrangement of isolated tetramers. In fact, 71% of the observed structures correspond to a network-like structure as the one illustrated in Fig. 8a, where, however, the additional water molecules connecting the trimers are still separated to a certain extent from the trimers. Interestingly, only 7% directly form the energy minimum structure shown Fig. 3c which is stabilized by the formation of two additional hydrogen bonds, reflected by the high differential adsorption energy for this particular water coverage structure demonstrated in Fig. 5. Obviously, the incorporation of the impinging water molecules into this chain-like structure is sterically hindered. The rest of the resulting water structures correspond to isolated tetramers, either in a square arrangement as illustrated in Fig. 8b, or in a rhomboidal shape .

For the surface with an initial water coverage of 4/9, the square-like water clusters connected by the fifth water molecule, illustrated in Fig. 3d, is the most frequently observed pattern within the Pt(111) 3×3 unit cell, about 35% of the resulting water structures correspond to this energy minimum structure. In the formation of this structure, the additional water molecule just needs to attach to the chain structure (Fig. 3c). In the remaining cases, more open two-dimensional water structures are formed as the one illustrated in Fig. 8c, which means that the initial water zigzag chain becomes broken.

This situation is different for water molecules hitting Pt(111) with an initial water coverage of 5/9 in the structure shown in Fig. 3d. Naively one would expect that the stable ice-like hexagonal water structure should form. However, indeed we have observed such an event only in 2% of the trajectories within the first 4 ps of the AIMD runs. The direct formation of a hexagonal ice-like structure is hindered by the fact that it requires the destruction of the tetramer motifs which is accompanied by the breaking of several hydrogen bonds.

Instead, pentagons connected by the sixth water molecule is the most frequently observed pattern (Fig. 9a) in 25% of the cases. In 10% of the events, three-dimensional structures form as the one illustrated in Fig. 9b, i.e., the impinging water molecule does not directly manage to become incorporated into a two-dimensional network as the initial structure is already rather dense. In the remaining cases, a variety of different two-dimensional structures forms. Often they consist of hexagons connected via pentagons or squares, but also octagons occur or a combination of pentagons and hexagons, as also observed as stable motifs on other metal surfaces [48, 49].

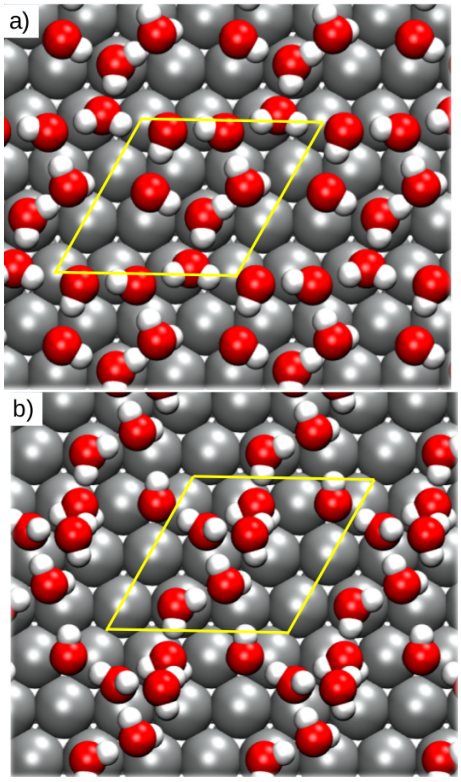

FIG. 9. Intermediate structural configurations formed for water molecules impinging on water pre-covered Pt(111) with an initial coverage of $\theta = 5/9$ resulting either in a connected pentagon pattern (panels a) or a three-dimensional arrangement (panel b).

IV. CONCLUSIONS

The adsorption dynamics of water molecules on Pt(111) has been studied by ab initio molecular dynamics simulations as a function of the initial kinetic energy and the water coverage on Pt(111). On clean Pt(111), the water sticking probability exhibits the typical behavior of molecular adsorption, it decreases with increasing initial kinetic energy. At low kinetic energies, the sticking probability is unity, at energies of about 0.2 eV, it has dropped to one half, at 0.4 eV it vanishes.

Initial water coverages from 1/9 to 5/9 within as a 3×3 surface unit cell lead to a significant increase in the sticking probability of impinging water molecules, in agreement with experimental observations. This is caused by a combination of the attractive water-water interaction with the additional effective energy dissipation channels provided by the adsorbed water molecules. The water structures forming directly after the adsorption do not necessarily correspond to energy minimum

structures. Either this is caused by steric hindrance or it occurs when the formation of the energy minimum structures requires a substantial rearrangement of the existing hydrogen-bonded network.

V. ACKNOWLEDGEMENT

Usual discussions with Charlie Campbell and Angelos Michaelides are gratefully acknowledged. This work has been supported by the German Science Foundation (DFG) through project GR 1503/25-1. Computational resources have been provided by the bwForCluster for computational and theoretical chemistry JUSTUS of the bwHPC project of the Federal State of Baden-Württemberg and by the Leibniz-Rechenzentrum (LRZ) of the Bavarian Academy of Science.

[1] P. A. Thiel and T. E. Madey, Surf. Sci. Rep. **7**, 211 (1987).
[2] M. A. Henderson, Surf. Sci. Rep. **46**, 1 (2002).
[3] A. Hodgson and S. Haq, Surf. Sci. Rep. **64**, 381 (2009).
[4] A. Groß, F. Gossenberger, X. Lin, M. Naderian, S. Sakong, and T. Roman, J. Electrochem. Soc. **161**, E3015 (2014).
[5] A. Michaelides, Appl. Phys. A **85**, 415 (2006).
[6] A. Roudgar and A. Groß, Chem. Phys. Lett. **409**, 157 (2005).
[7] K. Morgenstern and J. Nieminen, Phys. Rev. Lett. **88**, 066102 (2002).
[8] K. Andersson, A. Gómez, C. Glover, D. Nordlund, H. Öström, T. Schiros, O. Takahashi, H. Ogasawara, L. G. M. Pettersson, and A. Nilsson, Surf. Sci. **585**, L183 (2005).
[9] A. den Dunnen, M. J. T. C. van der Niet, C. Badan, M. T. M. Koper, and L. B. F. Juurlink, Phys. Chem. Chem. Phys. **17**, 8530 (2015).
[10] A. Michaelides and K. Morgenstern, Nature Mater. **6**, 597 (2007).
[11] M. Mehlhorn, S. Schnur, A. Groß, and K. Morgenstern, ChemElectroChem **1**, 431 (2014).
[12] R. Guidelli and W. Schmickler, Electrochim. Acta **45**, 2317 (2000).
[13] A. Michaelides, V. A. Ranea, P. L. de Andres, and D. A. King, Phys. Rev. Lett. **90**, 216102 (2003).
[14] S. Meng, E. G. Wang, and S. Gao, Phys. Rev. B **69**, 195404 (2004).
[15] S. Schnur and A. Groß, New J. Phys. **11**, 125003 (2009).
[16] S. Schnur and A. Groß, Catal. Today **165**, 129 (2011).
[17] J. Li, S. Zhu, and F. Wang, J. Mater. Sci. Technol. **26**, 769 (2010).
[18] J. Carrasco, B. Santra, J. Klimeš, and A. Michaelides, Phys. Rev. Lett. **106**, 026101 (2011).
[19] J. Carrasco, A. Hodgson, and A. Michaelides, Nat. Mater. **11**, 667 (2012).
[20] K. Tonigold and A. Groß, J. Comput. Chem. **33**, 695 (2012).
[21] J. Carrasco, J. Klimeš, and A. Michaelides, J. Chem. Phys. **138**, 024708 (2013).
[22] M. J. Kolb, F. Calle-Vallejo, L. B. F. Juurlink, and M. T. M. Koper, JCP **140**, 134708 (2014).
[23] M. J. Gillan, D. Alfè, and A. Michaelides, J. Chem. Phys. **144**, 130901 (2016).
[24] S. Sakong, K. Forster-Tonigold, and A. Groß, J. Chem. Phys. **144**, 194701 (2016).
[25] A. Groß, A. Eichler, J. Hafner, M. J. Mehl, and D. A. Papaconstantopoulos, J. Chem. Phys. **124**, 174713 (2006).
[26] W. Lew, M. C. Crowe, E. Karp, and C. T. Campbell, J. Phys. Chem. C **115**, 9164 (2011).
[27] S. Haq, J. Harnett, and A. Hodgson, Surf. Sci. **505**, 171 (2002).
[28] T. Panczyk, V. Fiorin, R. Blanco-Alemany, and D. A. King, J. Chem. Phys. **131**, 064703 (2009).
[29] T. Panczyk, V. Fiorin, and T. P. Warzocha, J. Chem. Phys. **133**, 034708 (2010).
[30] F. R. Laffir, V. Fiorin, and D. A. King, J. Chem. Phys. **128**, 114717 (2008).
[31] J. Behler, J. Phys.: Condens. Matter **26**, 183001 (2014).
[32] B. Hammer, L. B. Hansen, and J. K. Nørskov, Phys. Rev. B **59**, 7413 (1999).
[33] K. Forster-Tonigold and A. Groß, J. Chem. Phys. **141**, 064501 (2014).
[34] S. Grimme, A. Hansen, J. G. Brandenburg, and C. Bannwarth, Chem. Rev. , http://dx.doi.org/10.1021/acs.chemrev.5b00533 (2016).
[35] G. Kresse and J. Furthmüller, Phys. Rev. B **54**, 11169 (1996).
[36] S. Grimme, J. Antony, S. Ehrlich, and H. Krieg, J. Chem. Phys. **132**, 154104 (2010).
[37] E. R. McNellis, J. Meyer, and K. Reuter, Phys. Rev. B **80**, 205414 (2009).
[38] G. Mercurio et al., Phys. Rev. Lett. **104**, 036102 (2010).
[39] P. E. Blöchl, Phys. Rev. B **50**, 17953 (1994).
[40] G. Kresse and D. Joubert, Phys. Rev. B **59**, 1758 (1999).
[41] A. Groß and M. Scheffler, J. Vac. Sci. Technol. A **15**, 1624 (1997).
[42] A. Groß, Catal. Today **260**, 60 (2016).
[43] A. Groß, *Theoretical surface science – A microscopic perspective*, Springer, Berlin, 2nd edition, 2009.
[44] A. Groß, J. Chem. Phys. **135**, 174707 (2011).
[45] L. A. Mancera, R. J. Behm, and A. Groß, Phys. Chem. Chem. Phys. **15**, 1497 (2013).
[46] F. Gossenberger, T. Roman, and A. Groß, Surf. Sci. **631**, 17 (2015).
[47] H. J. Kreuzer, J. Chem. Phys. **104**, 9593 (1996).
[48] G. Revilla-Lopez and N. Lopez, Phys. Chem. Chem. Phys. **16**, 18933 (2014).
[49] L. Bellarosa, R. García-Muelas, G. Revilla-López, and N. López, ACS Cent. Sci. **2**, 109 (2016).